



## Technical note

## Accuracy of 3D surface scanners for clinical torso and spinal deformity assessment

Caroline A. Grant<sup>a,\*</sup>, Melissa Johnston<sup>b</sup>, Clayton J. Adam<sup>a</sup>, J. Paige Little<sup>a</sup><sup>a</sup>Paediatric Spine Research Group, Institute of Health and Biomedical Innovation at Centre for Children's Health Research, Queensland University of Technology, Brisbane, Australia<sup>b</sup>School of Chemistry, Physics and Mechanical Engineering, Queensland University of Technology, Brisbane, Australia

## ARTICLE INFO

## Article history:

Received 18 July 2017

Revised 19 October 2018

Accepted 5 November 2018

## Keywords:

3D Scanning

Scoliosis

Torso Deformity

Surface Deviations

Accuracy

Reproducibility of results

Surface topography

## ABSTRACT

Externally visible deformities are cosmetic features of great concern for Adolescent Idiopathic Scoliosis (AIS) patients. Current assessment techniques for AIS do not fully encompass the external deformity. A non-invasive method capable of capturing superficial anatomy, such as 3D scanning, would enable better qualitative and quantitative evaluation of cosmesis. This study aimed to quantify the accuracy of commonly available scanners, in assessing posterior asymmetry in AIS. The technique of 3D surface deviation analysis was proposed as a suitable method for comparing the models created by each scanner.

Eight plaster cast moulds manufactured to create braces for AIS patients were used as test samples. Four 3D scanners were selected: Solutionix RexScan CS+; Artec Eva; Microsoft Kinect V1; iPhone with 123D Catch App. These scanners were selected from those available as representative of a range of scanning technologies.

Each cast was scanned and 3D models created. A simulated rib hump measurement was obtained and the surface-to-surface deviations between the Solutionix scan and all other scans were determined. The Solutionix scanner is a metrology scanner of very high quality and so it was selected as the reference. Surface-to-surface deviations were calculated in the positive and negative directions separately to specifically identify size and volume inaccuracies created by the scans.

Surface deviations showed excellent agreement between the Solutionix and the Eva with deviations of  $+0.17 \pm 0.17$  mm (Eva regions larger) and  $-0.20 \pm 0.32$  mm (Eva regions smaller) (mean $\pm$ SD). The Kinect showed lower agreement ( $+1.58 \pm 1.50$  mm and  $-0.58 \pm 0.58$  mm). The iPhone scans were not able to be scaled to the correct size, so were excluded. Rib hump measurements with all scanners were within clinical measurement variability ( $\pm 4.9$  deg) of the known values.

These commercially available 3D scanners are capable of imaging torso shape in 3D and deriving clinically relevant external deformity measures. The non-invasive 3D topographic information provided can be used to improve assessment of torso shape in spinal deformity patients.

© 2018 IPEM. Published by Elsevier Ltd. All rights reserved.

## 1. Introduction

Adolescent Idiopathic Scoliosis (AIS) is typically thought of as a three-dimension deformity of the spine. The severity of the deformity is assessed using the Cobb angle [1] of the spine on a posterior-anterior radiograph. The change in the patients' Cobb angle over time can then be used to prescribe treatments – either operative or non-operative, and to assess the effectiveness of the chosen treatment. Using only the Cobb angle however, is an overly simplistic view of this condition, with the deformity being present

not only in the spine, but also in the rib cage creating a whole torso deformity.

It is this torso deformity which is often the first symptom observed by the patients or their parents – an uneven waist, hips or shoulders, a protruding scapula or protruding ribs above or below one breast. It is also this externally visible component of their condition that remains of great concern to patients and their parents [2], and its effect on patients health related quality of life is well documented [3].

Before the advent of easily accessible radiography for diagnosis of AIS the posterior component of the torso deformity, often called the rib hump, was considered a critical diagnostic indicator. Adam's forward bending test [4], described in 1865, is a method of examining a patients back while they were in a stooped posture in order to determine if they had a curvature to their spine.

Abbreviations: (AIS), Adolescent Idiopathic Scoliosis.

\* Corresponding author.

E-mail addresses: [ca.grant@qut.edu.au](mailto:ca.grant@qut.edu.au) (C.A. Grant), [m3.johnston@qut.edu.au](mailto:m3.johnston@qut.edu.au) (M. Johnston), [ca.grant@qut.edu.au](mailto:ca.grant@qut.edu.au) (C.J. Adam), [j2.little@qut.edu.au](mailto:j2.little@qut.edu.au) (J.P. Little).

**Table 1**  
Scanner details.

Scanner	Manufacturer	Technology	Stated accuracy	Scanner or sample handling	Retail price Scanner AU\$	Software processing manufacturer and costs
1 Eva	Artec Group Inc., Luxembourg	White light Structured light	Accuracy: up to 0.1mm	Hand held scanner, stationary sample, no limits or constraints to sample	\$25 000	Artec Studio v10, included in purchase price
2 Kinect V1	Microsoft Corp., Washington, USA	Infrared structured light	None stated, not original purpose	Hand held scanner, stationary sample, no limits or constraints to sample	\$250	Free software “3D Scan app” now available from Microsoft for Windows 10 (Note: Artec Studio used in this study v10)
3 123D Catch (iPhone app)	AutoDesk Inc., California, USA	Photogrammetry	None stated	Hand held scanner, stationary sample, scan volume limited by total photo upload of 60 images	\$0 (+users Apple iPhone 6s with 12MP camera (Apple, California, USA))	Free, processed online by Autodesk
4 Rexcan CS+	Solutionix, Seoul, Korea	Blue LED structured light	None stated	Fixed desktop scanner, sample mounted on an automated turn table, small scan volume	\$60 000	Built in processing, included in purchase price

Today this method of diagnosis continues as an initial examination test prior to referring the patient for radiographs. The test itself has changed little, though a specialised goniometer or protractor, commonly a Scoliometer, has been added to quantify the size of the rib hump or rotational deformity [5]. Additionally several questionnaires have been developed to help document the patients perception of their torso deformity including the Walter Reed Visual Assessment Scale [6] and the Trunk Appearance Perception Scale [7].

While the measurement of the rib hump is standardly included in clinical assessment of a patient, the size or meaning of this measurement is often not considered. While surgeons acknowledge that aesthetics is of primary concern in AIS surgery [8], the primary outcome measure in assessing surgical correction of AIS is the reduction in the Cobb angle. However it has been shown that this measure of success has little correlation to patient satisfaction with their surgery [9–11]. Perhaps a more comprehensive measure of full torso deformity would have a greater correlation.

In the past attempts have been made to quantify the torso rotational deformity in greater detail, most prominently using Moiré topography [12]. This technique used the projection of lines onto the patients back to quantify the asymmetry. Logistically however, this technique proved difficult to setup and so was not widely adopted. More recently 3D scanning using structured light scanners has started being used for research into the AIS torso deformity [13–26].

3D models offer the ability to capture the full geometry of the patient. Calculations of asymmetry on anterior and posterior surfaces as well as changes with time are able to be compared. These 3D scans show great potential in recording, measuring and tracking the external deformity in patients [23,24].

The technology and availability of 3D scanners however are changing rapidly and with them comes the question of which of the available scanners are best suited to a clinical application? This study examined four commercially available 3D scanners, at a variety of price points, and using a variety of different scanning technologies, to determine the accuracy of the scanners in replicating a 3D object, and the ability of the scans captured to be used to recreate the clinical measurement of rib hump using a Scoliometer.

A 3D linear or surface to surface deviation analysis was used to compare the 3D model surfaces generated by each scanner. This technique provides a powerful tool to compare surfaces either

when assessing different technologies for generating the surface, or for comparing differences between two objects, or changes in the same object at different time points. This technique has been used previously to assess wear of medical implants [27] and is used in manufacturing quality assurance processes [28]. Similar techniques have also been used previously to assess the effect of CT image segmentation techniques and the accuracy of MRI generated models of bones [29,30] and in examining the symmetry of scoliosis patients [17,19,23,24].

## 2. Methods

### 2.1. Scanners

Four scanners were selected for inclusion in this study (Table 1), with three of these representing technologies which could feasibly be implemented in a clinical environment. These three scanners were selected to represent a range of technologies and price points from those available commercially (as detailed in Table 1). The fourth scanner, Solutionix Rexcan CS+, is a fully calibrated blue LED metrology scanner capable of automatically scanning and reconstructing a small desktop volume (Ø300mm x 215 mm). This scanner is not appropriate for use in the clinical setting as it is a non-portable fixed scanner, but was included instead as the ‘Gold Standard’ for measurement of the samples due to its superior scanning accuracy. The Rexcan C+ uses ultra-high accuracy structured light scanning technology, whereby a blue light pattern (grid type) is projected onto the surface of interest and multiple cameras capture the distortion of this pattern from different orientations. The distance to each of these points is calculated and the three-dimensional position of these points used to reconstruct the surface geometry. By comparing many thousands of points, the reconstructed geometry has an exceptional level of detail and very high precision. The blue LEDs used have a very short wavelength and are highly coherent giving the scanner the highest possible accuracy. Both the Artec Eva scanner and the Microsoft Kinect v1 scanner also use structured light as their means of creating a 3D model, however they each utilise a different light source, white light (Eva) and infrared (Kinect). These alternate light sources reduce the achievable accuracy of the reconstructed scan. The iPhone app uses photogrammetry to create its 3D models, using information taken from dozens of photographs of the object to reconstruct the geometry [31].



**Fig. 1.** A plaster cast mould of the posterior torso of an AIS patient. Casts made in the process of bracing the patients were replicated for use in a previous study on the use of an iPhone as a substitute Scoliometer [32], and were used as models for assessing 3D scanners in the present study. The calibration tool is visible attached to the left side of the mould.

## 2.2. Samples

Eight plaster cast moulds of the posterior torso of AIS patients were used as models for scanning (Fig. 1). These casts were created during the process of brace creation for the patients and have been used previously in the validation of the iPhone (with acrylic sleeve) as a substitute Scoliometer, and so have a known rib hump (mean  $16^\circ \pm 5.8$  (range 6–30)) [32]. The casts are positive replicas of the patient's external torso anatomy at true to life size. Each plaster cast is covered in a 7 mm thick layer of foam (EVA), to mimic the skin surface.

A calibration tool (3D printed in ABS) was attached to the side of each cast (Supplementary Fig. 1), to act both as a consistent reference from which to create a reliable coordinate system between scans and also to quantify the ability of each scanner to accurately detect and reconstruct geometric shapes of various types and sizes. While humans are not made of simple geometric shapes, the inclusion of each of the shape types in this object (sphere, cylinder, cone and cube) enabled the scanners limitations to be examined in a controlled manner. Rounded shapes (sphere, cylinder and cone) were emphasised for their basic similarity to organic features, with each at risk of scanning errors due to incorrect registration of images. To quantify the ability of the scanners to replicate these shapes, the surfaces corresponding to each shape were selected and the appropriate geometric shape was fitted (automatic best fit) to the surface and its parameters recorded.

## 2.3. Scans

The plaster casts were scanned using each of the four scanners. For the Solutionix scanner this was an automated process in which the cast was mounted to a computer controlled rotating and tilting platform, the cast was then scanned repeatedly in numerous orientations until a complete model was created. All other scans were conducted manually by a single author (CG). Eva and Kinect scans were both conducted using Artec studio (v10 Professional, Artec Group Inc., Luxembourg) image processing software. To capture the scans, the hand held Eva and Kinect scanners were (individually) pointed at the cast, while user walked around the cast, monitoring the scanned area displayed on screen to ensure the full

volume was captured. For 123D Catch, a series of 40–70 photographs were captured of the cast covering the full volume, using the authors' iPhone 6. The photographs, captured in the app, were then automatically processed using photogrammetry techniques by AutoDesk via internet based submission through the app. A 3D model of the cast was then available for download after the processing. In each case the final scan obtained from each device was exported in .stl format for post-processing.

## 2.4. Analysis

Each scan was imported into Geomagic Wrap (2015, 3D Systems, North Carolina, USA) for cleaning and removal of unwanted additional items captured in the background of the scan. For the Kinect and 123D catch scans this process involved use of the mesh doctor and global smoothing tools. The mesh doctor is a built in automated process for cleaning scan data. It includes correction or removal of Non-Manifold Edges, Self-Intersections, Highly Creased Edges, Spikes, Small Components, Small Tunnels and Small Holes. Global smoothing was applied using the Quick Smooth command. There are no options or parameters associated with either of these commands.

Because of the risk of over smoothing and losing detail, smoothing was only performed when considered absolutely necessary. Scans from the Solutionix and Eva were used in their raw state as exported from the capture software, with only the removal of unwanted regions of the scans.

Figures showing the raw scans, the cleaned scans and a 3D linear deviation analysis between them for the Kinect and 123D catch are included in supplementary Fig. 2.

Once cleaned, all four scans for a single torso mould were imported into Geomagic Control (2015, 3D Systems, North Carolina, USA) for comparison. A local coordinate system was created in the Solutionix scan, such that the table on which the cast was placed formed the x-y plane, a cylindrical axis of best fit along the length of the torso was then used to define the direction of the x-axis along this plane, and the location of the centre of the calibration tools' sphere was set as the origin. This created cross sections aligned in the y-z plane, perpendicular to the longitudinal axis of the plaster cast and therefore, the patient's torso. All other torso casts were then automatically registered to each other using a global registration process. This in-built algorithm uses a least squares method to minimise the distance between the two surfaces across the entire model, shifting the scanner test models to the Solutionix model with the created coordinate system.

A 3D linear deviation analysis was then conducted between the scans created using the Solutionix scanner and scans from the other three scanners, such that a positive deviation occurred when the test scan was larger than the Solutionix scan, and vice versa for a negative deviation. Deviations were assessed across the whole surface of the scans. In this automated process in Geomagic Control, the 3D linear vector distance between each point on the test scan (Eva, Kinect or 123D catch) and the closest corresponding point on the reference scan (Solutionix scan) was calculated. Full deviation maps and results tables (ie the result from every point on the test scan) were exported for further analysis in Excel (Microsoft Corp., Washington, USA). Sectioned views aligned in the y-z plane were then taken through each cast at 20 mm intervals along the x-axis (Fig. 2). Within each of these slices the linear deviations were assessed and the mean and standard deviation of the positive and negative deviations were assessed. Regions corresponding to the calibration tool were specifically excluded due to any possible errors in reproducing its geometry.

Simulated rib hump measurements were also calculated at each slice location and the largest value seen across the torso reported

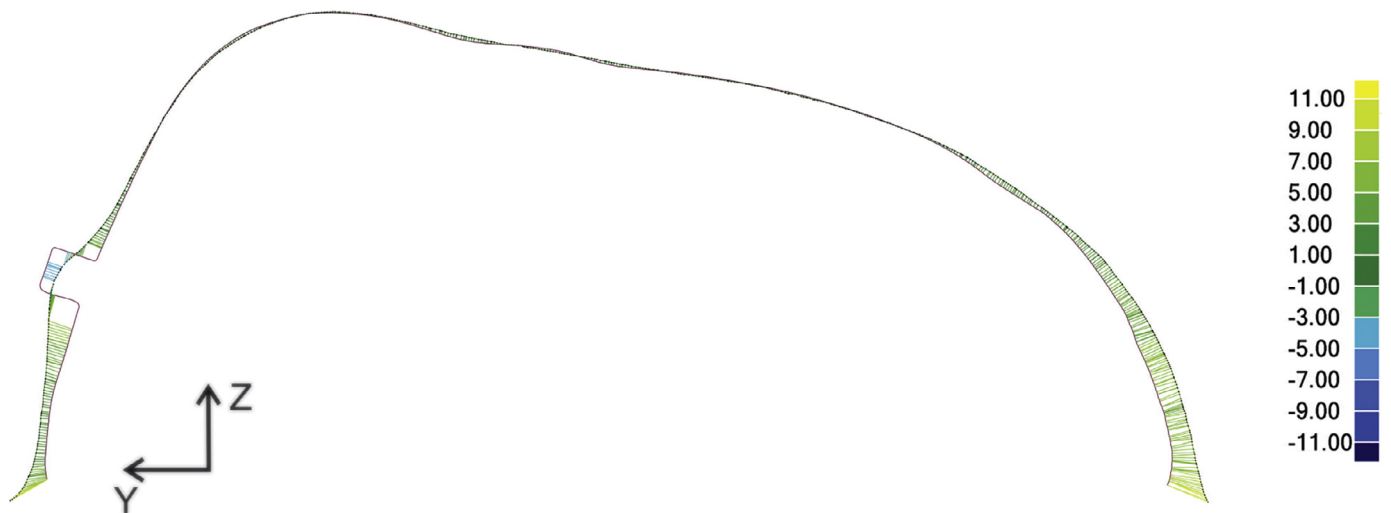


**Fig. 2.** Slice ( $y$ - $z$  plane) through two scans, Solutionix in red, and Microsoft Kinect in black, showing the linear deviations between them (yellow, green and blue whiskers). The scale shows deviations from +11.00 mm (yellow) to -11.00 mm (blue). Note that a negative deviation occurs when the test scan (Microsoft Kinect in this case) lies inside the reference scan (Solutionix), and a positive deviation where it is outside the reference scan. Both of these cases can be seen on the left of the image surrounding the calibration tool. (For interpretation of the references to color in this figure legend, the reader is referred to the web version of this article.)

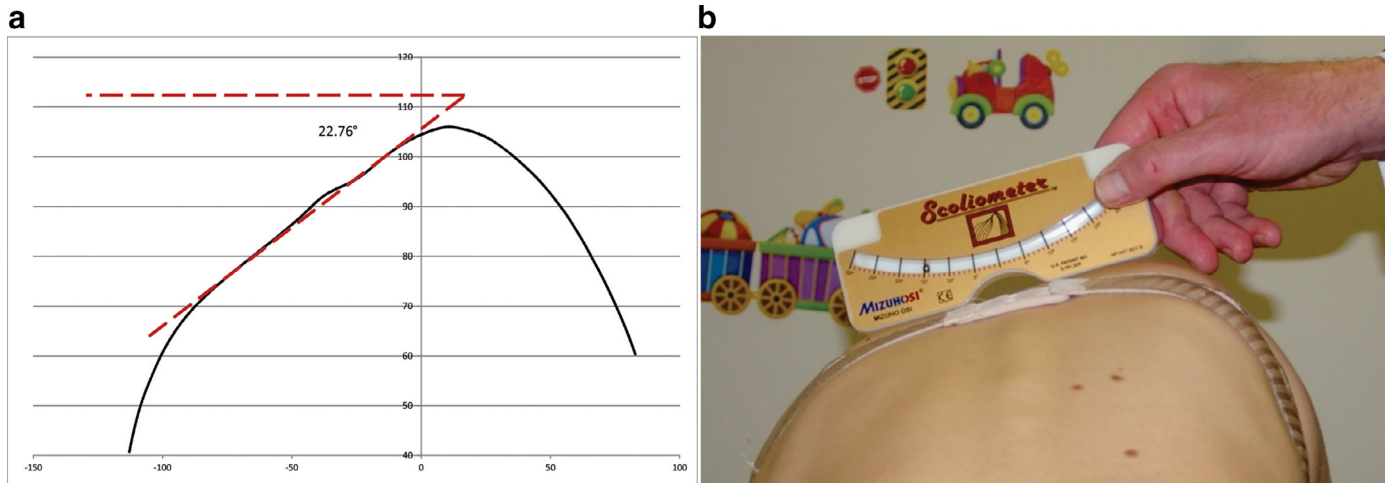


**Fig. 3.** (a) Calculation of a simulated rib hump from a  $y$ - $z$  plane slice through a Solutionix scan, note the spinous process excluded from the fitting requirements (b) use of a Scolometer to measure Rib Hump clinically.

as the measured rib hump for that scanner for that cast. The simulated rib hump was calculated as the angle of the steepest line tangential to the scan, making contact on both sides of the spinous process (Fig. 3a). In this way the central cut out of a traditional Scolometer (National Scoliosis Foundation, Watertown, MA, USA) was simulated (Fig. 3b), while calculating this within the  $y$ - $z$  plane slices ensured that the measurement was performed perpendicular to the longitudinal axis as would be done clinically [5]. Comparison was then made to the clinical measurement of rib hump as obtained by experienced clinicians with a Scolometer [32]. The Scolometer has been shown to have excellent inter- and intra-rater reliability in the mid to lower thoracic region [33]. Inter-rater mean differences are reported to be as high as  $1.1^\circ$ , with 95% confidence intervals of  $\pm 4.9^\circ$  [32–34].

The scanned dimensions of the calibration tool geometric components were determined by fitting standard shapes to the scanned surfaces. Comparisons were then made between the designed dimensions of the object and the diameter of the sphere, the diameter of the cylinder, the angle of the cone (half the angle enclosed between the sides), and the planar distance between two opposing surfaces of the cube as shown in Supplementary Fig. 1.

### 3. Results

Thirty one of a possible thirty two scans were obtained. Difficulty was experienced in scanning one of the torso casts with the 123D catch app on the iPhone, and after several repeat attempts (different locations and lighting) this scan was abandoned. It is not clear why this scan repeatedly failed. All other torso casts were successfully scanned with all scanners. Examples of each of the four scans for a single torso cast are shown in Fig. 4.

Additionally, the seven scans that were captured with the 123D Catch iPhone app were all lacking in scale information - the torso scans generally appearing to be  $\sim 1/10$ th or less of actual size. Attempts were made to scale the scans using the calibration tool, however this proved unsuccessful due to the limited resolution of the scans (Fig. 4D). For this reason the scans obtained with the 123D catch app have been removed from the remaining analysis. Approximate length and width measurements of the actual casts and the 123D catch models are included in the raw and processed scan images in supplementary Fig. 2.

Cleaning of the raw scans is an important part of the process of obtaining a usable model. There is a risk however of over

**Table 2**

Comparison of the calibration tools dimensions from the Solutionix and Eva scanners vs. the original design dimensions.

	Sphere diameter (mm)	Cylinder diameter (mm)	Cone Half angle (°)	Cube width (mm)
Designed size	20.00	15.00	30.00	10.00
Solutionix (Mean ± St Dev)	20.06 ± 0.09	15.02 ± 0.07	29.03 ± 1.25	9.98 ± 0.07
Eva (Mean ± St Dev)	20.17 ± 0.43	15.19 ± 0.63	28.56 ± 1.66	9.70 ± 0.92

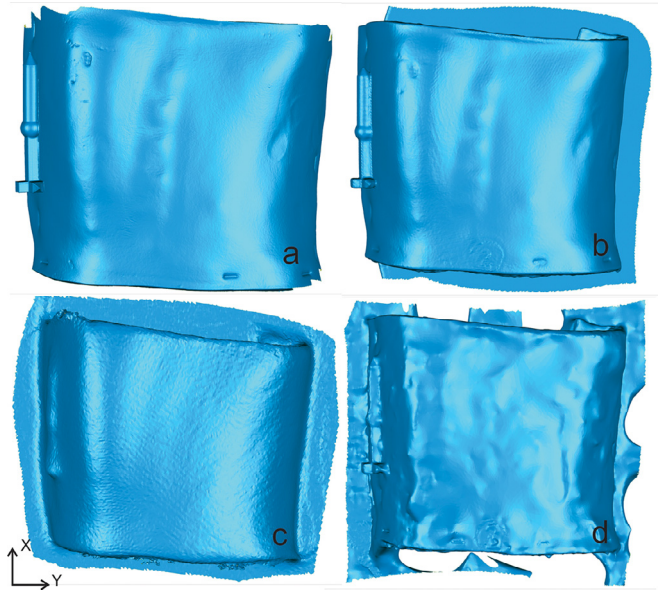


**Fig. 4.** Images of processed scan data (A) Solutionix Rexcan CS+; (B) Artec Eva; (C) Microsoft Kinect V1; (D) 123D Catch iPhone App; all raw data images can be seen in supplementary Fig. 2.

smoothing the model in pursuit of a more visually appealing model and in the process losing important details or changing the overall dimensions of the model. To quantify the effects of the clean process on the Kinect and 123D catch models a 3D linear deviation analysis was performed between each raw model and the processed clean model. Figures showing the raw, clean and deviation analysis for each scan are available in supplementary Fig. 2. For the Kinect scanner the largest average deviation within a scan caused by cleaning was 0.065 mm. For the 123D catch scans the issue of the overall size of the raw models prevents a useful calculation of deviations

### 3.1. Calibration tool comparisons

The dimensions of the scanned calibration tool were compared to their original designed dimensions by fitting the geometric shape to the appropriate region of the scanned surface (Table 2). As the object was 3D printed however the true final dimensions of the object are not known. The 5 geometric shapes were not able to be fit to any of the Kinect models due to the low resolution of the obtained scans. For example the region corresponding to the sphere in the centre of the calibration tool could not be identified in order to fit a geometric sphere to it.

### 3.2. Rib hump

The simulated Rib hump values were compared to those measured by experienced clinicians using a Scoliometer, as reported previously in the literature for these casts [32]. The angular difference to each of the four scanners is shown in Table 3.

### 3.3. Surface deviations

Linear surface deviations are reported in comparison to the Solutionix scanner in each case in Table 4, Fig. 5. A positive deviation occurred when the test scan was outside the Solutionix scan, and vice versa for a negative deviation. Both positive and negative deviations can be seen in Fig. 3 surrounding the calibration tool, with the blue whiskers showing a negative deviation, and the green-yellow showing a positive deviation.

## 4. Discussion

While more researchers and clinicians are embracing the use of 3D scanning in clinical applications, the appropriateness of their choice of scanner in each case has not been assessed. There are an ever increasing number of 3D scanners available commercially these days. This paper aimed to determine the accuracy of a few commercially available scanners at a range of price points, in both linear surface deviations and clinically relevant angular measurements (Rib Hump). The scanners chosen also represent two basic technologies – structured light scanners and photogrammetry, with three light source variations in the structured light scanners (Blue LED, White light and Infrared).

In researching scanners for this investigation it became clear that manufacturers do not like to give values for the achievable levels or accuracy or precision of their scanners. As was noted in Table 1, of the scanners included in this study, only the Artec Eva has a reported accuracy. This makes scanner comparison challenging for consumers.

In a structured light scanner, the quality of the light source is fundamental to the achievable accuracy of the scanner. Blue LEDs are the industry gold standard for this purpose. LEDs are monochromatic and provide a highly coherent light source, combined with the choice of blue light, having the smallest wavelength available means the projected ‘structured light’ pattern is of very high quality, and has a very low susceptibility to external lighting and conditions. This in turn means the captured images and calculated depth of each part of the image is of a very high quality. White light from a standard flash bulb, as used by the Eva, in contrast covers the full spectrum of visible wavelengths. This lowers the quality of the projected pattern on the object. Additionally visible light and heat (infrared) from external sources can create noise or artefacts and lowers the quality of the final 3D model. Though as seen in this work, the differences between the Eva and the Solutionix scans are generally quite small in this context. The Microsoft Kinect, rather than using visible light, uses infrared. Infrared light has an even greater susceptibility to degradation by external sources of heat. This again lowers the achievable quality of the scan.

Scans captured by the 123D catch app had to be removed from the analysis due to a lack of scale information. This is unfortunate as the technique used by the app – Photogrammetry, is widely used in other engineering and scientific applications with good quality results. In this instance there was the possibility of using the calibration tool to scale the final models; however the extremely low resolution of the scans produced created large errors in this scaling which would have confounded all other geometric comparisons. Being a free application, with cloud based processing

**Table 3**  
Scoliometer published values [32], and the difference in maximum Rib Hump angle (degrees) between each scanner and the Scoliometer values.

Sample	Scoliometer measured value	Difference between scan and Scoliometer value (°)		
		Solutionix	Eva	Kinect
Torso 1	17.10	0.24	0.67	0.33
Torso 2	12.10	1.01	1.11	1.98
Torso 3	25.60	0.99	1.06	−1.89
Torso 4	9.70	−0.56	0.06	−0.66
Torso 5	9.60	0.46	0.63	0.04
Torso 6	19.40	3.55	3.37	2.85
Torso 7	19.20	0.85	1.44	0.11
Torso 8	11.90	−0.40	−0.61	−0.51
Mean		0.77	0.96	0.28
Standard Deviation		1.27	1.17	1.50

**Table 4**  
Linear surface deviations (mm).

Scanner	Positive deviations			Negative deviations		
	Mean	Standard deviation	Mean number of points	Mean	Standard deviation	Mean number of points
Artec Eva	0.17	0.17	4035	−0.20	0.32	2513
Microsoft Kinect	1.58	1.50	4277	−0.58	0.58	819

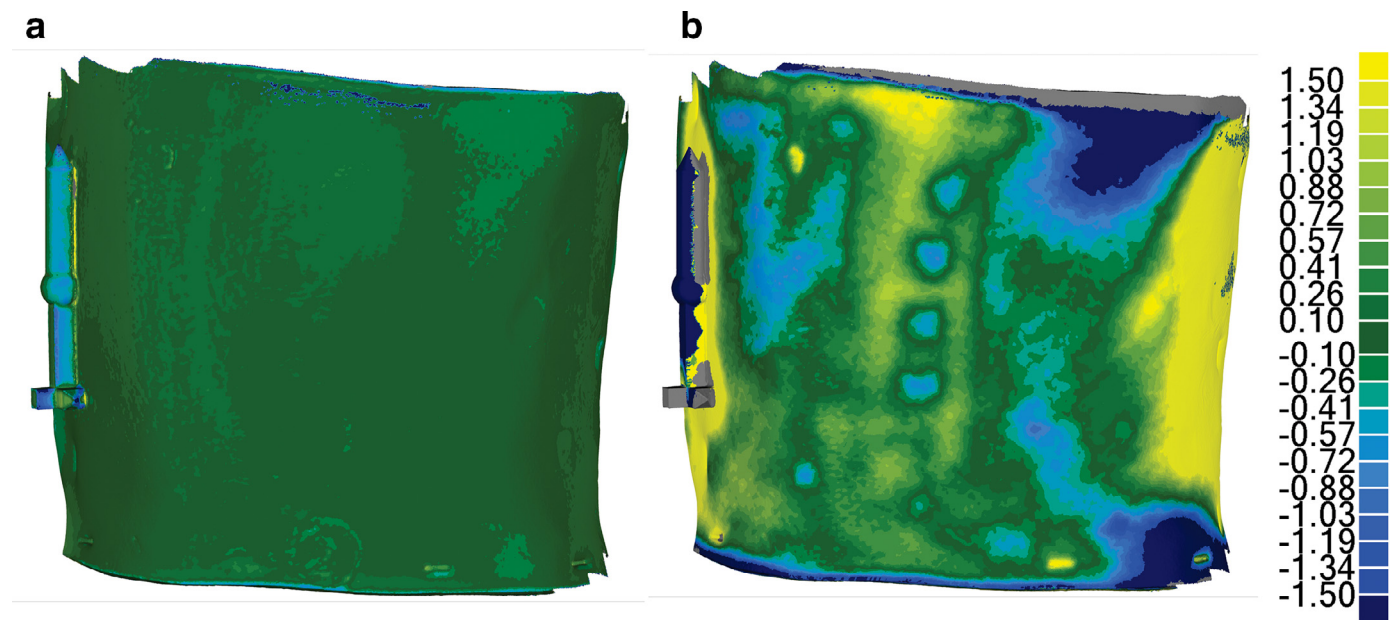


**Fig. 5.** Surface deviation maps for an individual torso mould (a) Solutionix vs Artec Eva; (b) Solutionix vs Microsoft Kinect; deviations from +1.5 mm (yellow) to −1.5 mm (blue). (For interpretation of the references to color in this figure legend, the reader is referred to the web version of this article.)

of images resulted in a very limited point cloud resolution of the final model. Using photogrammetry techniques with higher quality software processing and image quality would likely alleviate this issue and the inclusion of a scaling object would then allow high quality, correctly sized models to be created.

Additionally, this app or ones of a similar nature using online or cloud based external processing of images raise privacy issues when considering clinical datasets.

For linear deviations in comparison to the Solutionix REXCAN CS+ scanner, the other three scanners performed with varying results. The Artec Eva scanner performed well, achieving the lowest deviation in both the positive and negative directions at  $+0.17 \pm 0.17$  mm and  $-0.20 \pm 0.32$  mm, respectively. While the size of these deviations is roughly equivalent, the mean number of points occurring in each direction shows a slight bias towards creating a larger model than that seen by the Solutionix. The accuracy of scans obtained with the Eva scanner makes it ideally suited to clinical applications in which fine detail is necessary.

The Microsoft Kinect performed less well, though with a substantially cheaper price point this is probably to be expected. Deviations of  $+1.58 \pm 1.50$  mm and  $-0.58 \pm 0.58$  mm show a strong bias to the creation of a larger model, with less dimensional accuracy. With this level of accuracy, small anatomical features could easily be lost in a clinical setting. There was also a tendency for these models to be shorter longitudinally (in the x-direction), this is evident in Supplementary Fig. 4 with the grey and dark blue regions along the top and bottom edge of the cast being areas where the Kinect model was too far away from the reference model to be included in the assessment, i.e. there was no surface to compare to, and is shown in Supplementary Fig. 2, with the Kinect and Solutionix models overlaid. A total length difference such as this is likely due to the physical and optical smoothness of the foam covering of the torso casts. The lack of optical texture/features at the resolution of this scanner creates registration errors between frames during the scanning process, making them overlap by a larger degree than is correct, causing the model to

shorten. In the clinical setting when scanning skin, which is highly optically textured however, this problem would be minimised. Adding a matt finish to the surface or a speckled, spotted or variegated colour pattern to the surface would also assist in the optical tracking of the object.

The Kinect models were also seen to have small linear deviations across the flatter central regions of the model (the 'top' surface in the y-z slices), with the region at the sides of the chest flaring wider than the reference model creating the large positive deviations that were seen (Fig. 2 and yellow regions in Fig. 5b). Again this could be caused by scanning registration errors resulting in a model significantly wider than the actual object.

In contrast to linear deviations, the angular Rib hump measurements were much more reliable, particularly in the context of the clinical repeatability of this measurement (inter-rater mean difference 1.1°, 95% CI 4.9°) which includes confounding factors of the movement of the patient and patient variability in performing the forward bend test repeatedly. The Solutonix, Eva and Kinect scanners all showed greater accuracy than clinical levels in all scans. Though the number of torso casts included in this study was small at only 8, they included a wide variety of curve types, locations and severity as would be seen clinically. Both the Eva and Kinect scanners were able to replicate the Scoliometer value for each torso cast within the range of clinical accuracy.

Comparison of the calibration tools' scanned dimensions and their original designed dimensions showed that both the Solutonix and Eva scanners are good at replicating round or spherical surfaces with the smallest differences seen in the Sphere and Cylinder diameters. The cone presented a problem to both scanners because of its tapering point, which was rounded off or obscured by shadows and the inability of the scanners to adequately see under the object. The cube was replicated well by the Solutonix, but the Eva scans suffered from rounding of the corners leading to a smaller measured size. In contrast the calibration tool was not well enough replicated by the Kinect scanner to test any of the shapes. As can be seen in Fig. 4C (in results), only a vague outline of the tool is seen in the scan. This could be problematic if the application requires capture of even relatively large features on the surface of an object.

The linear deviation analysis provided a robust technique for visually and numerically assessing the differences between two objects. The deviation maps were able to clearly show the location and magnitude of differences, enabling the determination of the causes of those differences.

To extend this technique into the clinical setting of measuring real human torsos a number of factors would need to be considered and methodology developed to achieve high quality scans with useable clinical measures. While there are a number of challenges associated with introducing these techniques clinically, there are also great advantages. Real patients will move throughout the scans, both breathing and swaying will occur during the time course of a scan and these will cause artefacts that will need to be dealt with in a consistent way.

For quantification of the rib hump, a patient could be positioned in a traditional Adam's forward bend, and their back scanned. However in contrast to a single Scoliometer measurement, a 3D scan would allow for much greater detail in the data captured and stored. This would then enable closer comparison and monitoring of the patients external torso deformity over time. Comparing scans at different time points however raises challenges of consistency of positioning and methods of comparison of two similar but potentially quite different objects as patients undergo both normal growth and progression of their deformity.

A number of papers have been published from a Canadian group utilising surface topography to monitor scoliosis in the clinical setting, and in comparison to skeletally healthy adolescents

[17,19,23,24]. Their use of a symmetry analysis for quantifying the curve magnitude and monitoring progression is an interesting application of these techniques to the clinical setting. Their scanner however is not a commercially available product (though it is comprised of commercially available cameras etc.), and no information is given on the achievable geometric accuracy of the acquired scans. As noted throughout this study though, when examining the gross geometry of the torso and the changes which occur in a condition such as scoliosis, the required geometric accuracy of the models is much lower than would be required in other applications.

#### 4.1. Limitations

The torso casts used in this study were covered in a white foam layer. This material is not ideal for 3D scanning purposes and is not particularly similar to human skin. Human skin is an ideal material for 3D scanning as it contains lots of visual texture (veins, hair, freckles, moles etc.). For this reason each of the scanners considered in this study would likely perform better when examining a human than they did when examining these casts, so these results can likely be taken essentially as a worst case scenario.

While the number of casts included in the study is small at only eight. They represent a wide variety of AIS curve types, locations and severities on a range of different sized people (the approximate dimensions of the torso casts can be seen in the supplementary figures).

Each of the torso casts were only scanned once, and all by a single investigator. Hence no comment can be made on the repeatability of the scans or any variations that different investigators might introduce.

These scanners used in this study were selected because of their availability for inclusion in the study and because they represented a range of technology types and price points. There are many other commercial scanners available with more being brought to market daily, and as such it is simply not feasible to compare all of the available scanners. As noted in the results of this study, care should be taken when selecting a scanner to ensure that the results that are achievable meet the requirements of the intended application.

Neither scan time nor processing time were captured in this investigation. In a clinical setting, both of these parameters would be of importance. With a hand held scanner such as the ones used in this investigation, the time taken to capture a whole body 3D scan would be a matter of a few minutes, depending on the frame rate of the specific scanner. The specific data processing used in this study is not proposed as a clinical methodology. In a clinical setting, automated algorithms should be produced to calculate any parameters of interest.

Additionally, only a single clinical measurement was included in the study, however this is representative of the typical clinical examination of a scoliosis patient in which the single rib hump measurement is the only external measurement taken.

## 5. Conclusion

3D scanning has great potential in clinical applications, but care is needed in selecting the appropriate scanner. Some applications, such as scanning facial features, require a very high geometric accuracy (<0.5 mm), while others, such as brace or orthotic design; require volumetric accuracy to ensure comfort and efficacy of the created brace. In these applications a white light structured light scanner such as the Artec Eva is ideally suited. Collection of simple angles and distances between anatomical landmarks on the other hand may be able to be collected with lower accuracy ( $\pm 1-5$  mm) without excessive clinical risk, for example with a Microsoft Kinect,

though repeated collection over time for example to assess growth or changes in a condition, may require higher levels of accuracy, or the acceptance of larger thresholds for measuring a change in the parameter.

While relatively more expensive (\$25,000), the Artec Eva scanner showed superior performance in linear deviations with submillimetre accuracy obtained and Rib Hump angles well within clinical repeatability. From these results, of the four scanners compared this would be the recommended scanner for use in clinical applications involving fine anatomical detail, or volumetric accuracy. This scanner uses a white light flash bulb as its structured light source.

For applications requiring less anatomical detail or where a global size overestimation is not considered a problem, the Microsoft Kinect provides a simple low cost scanner for rapidly capturing gross anatomical parameters. Caution should be used though if linear or area measurements are required as the model is likely to be significantly larger than the scanned object.

The 123D catch iPhone app should only be used with caution. Measurements should not be taken from these scans as scaling information is unreliable even with the inclusion of a calibration object. The basic technique of photogrammetry used by the app however remains a viable option if higher performing software and photography are used [31].

The 3D linear deviation analysis technique used provided a powerful tool for comparing two surfaces. As well as being used to assess the differences between scanning technologies, this technique also has applications in assessing errors or inaccuracies from different imaging modalities (such as CT to MRI 3D volume comparison), differences between similar objects (e.g. left/right symmetry assessment of bones or limbs), or changes in an object over time (e.g. growth or deformity progression).

Manufacturers of 3D scanners will rarely report the achievable accuracy of their devices. This paper compared three structured light scanners with differing light sources and one photogrammetry scanner. With Blue LED scanners being the industry standard for high accuracy measurement, a scanner using this technology will produce 3D models of very high fidelity but is likely to come at a much higher price point. The white light scanner used in this study produced models of only slightly lower quality but at less than half the price.

## Acknowledgements

We wish to pay tribute to a valued member of our Spine Research Group, Professor Clayton James Adam who died on March 6, 2018 and will be forever missed by the team.

The authors would like to acknowledge the High Performance Computing and Research Support Group at Queensland University of Technology, for the computational resources and services used in this work.

## Conflicts of interest

None.

## Funding

This research was supported by funding from Queensland University of Technology and group operating support provided by Synthes, Medtronic and the Mater Foundation.

## Ethical approval

Not required.

## Supplementary materials

Supplementary material associated with this article can be found, in the online version, at doi:[10.1016/j.medengphy.2018.11.004](https://doi.org/10.1016/j.medengphy.2018.11.004).

## References

- [1] Cobb JR. Outline for the study of scoliosis. In: Edwards JW, editor. *Instructional course lectures Vol 5*. Ann Arbor, MI: American Academy of Orthopaedic Surgeons; 1948. p. 261–75.
- [2] Bridwell KH, Shuffelbarger HL, Lenke LG, Lowe TG, Betz RR, Bassett GS. Parents' and patients' preferences and concerns in idiopathic adolescent scoliosis: a cross-sectional preoperative analysis. *Spine (Phila Pa 1976)* 2000;25:2392–9. doi:[10.1097/00007632-200009150-00020](https://doi.org/10.1097/00007632-200009150-00020).
- [3] Tones M, Moss N, Polly DW. A review of quality of life and psychosocial issues in scoliosis. *Spine (Phila Pa 1976)* 2006;31:3027–38. doi:[10.1097/01.brs.0000249555.87601.fc](https://doi.org/10.1097/01.brs.0000249555.87601.fc).
- [4] Adams W. *Lectures on the pathology and treatment of lateral and other forms of curvature of the spine*. London: Churchill; 1865.
- [5] Bunnell WP. An objective criterion for scoliosis screening. *J Bone Joint Surg Am* 1984;66:1381–7.
- [6] Sanders JO, Polly DW, Cats-Baril W, Jones J, Lenke LG, O'Brien MF, et al. Analysis of patient and parent assessment of deformity in idiopathic scoliosis using the Walter Reed Visual Assessment Scale. *Spine (Phila Pa 1976)* 2003;28:2158–63. doi:[10.1097/01.BRS.0000084629.97042.0B](https://doi.org/10.1097/01.BRS.0000084629.97042.0B).
- [7] Bago J, Sanchez-Raya J, Perez-Grueso FJS, Climent JM. The Trunk Appearance Perception Scale (TAPS): a new tool to evaluate subjective impression of trunk deformity in patients with idiopathic scoliosis. *Scoliosis* 2010;5:6. doi:[10.1186/1748-7161-5-6](https://doi.org/10.1186/1748-7161-5-6).
- [8] Negrini S, Grivas TB, Kotwicki T, Maruyama T, Rigo M, Weiss HR. Why do we treat adolescent idiopathic scoliosis? What we want to obtain and to avoid for our patients. SOSORT 2005 Consensus paper. *Scoliosis* 2006;1:4. doi:[10.1186/1748-7161-1-4](https://doi.org/10.1186/1748-7161-1-4).
- [9] Wilson PL, Newton PO, Wenger DR, Hafer T, Merola A, Lenke L, et al. A multicenter study analyzing the relationship of a standardized radiographic scoring system of adolescent idiopathic scoliosis and the Scoliosis Research Society outcomes instrument. *Spine (Phila Pa 1976)* 2002;27:2036–40. doi:[10.1097/00007632-200209150-00013](https://doi.org/10.1097/00007632-200209150-00013).
- [10] D'Andrea LP, Betz RR, Lenke LG, Clements DH, Lowe TG, Merola A, et al. Do radiographic parameters correlate with clinical outcomes in adolescent idiopathic scoliosis? *Spine (Phila Pa 1976)* 2000;25:1795–802. doi:[10.1097/00007632-200007150-00010](https://doi.org/10.1097/00007632-200007150-00010).
- [11] Koch KD, Buchanan R, Birch JG, Morton AA, Gatchel RJ, Browne RH. Adolescents undergoing surgery for idiopathic scoliosis: how physical and psychological characteristics relate to patient satisfaction with the cosmetic result. *Spine (Phila Pa 1976)* 2001;26:2119–24. doi:[10.1097/00007632-200110010-00015](https://doi.org/10.1097/00007632-200110010-00015).
- [12] Takasaki H. *Moire Topography from its birth to practical application*. *Opt Lasers Eng* 1982;3:3–14.
- [13] Gorton GE, Young ML, Masso PD. Accuracy, reliability and validity of a 3D scanner for assessing torso shape in idiopathic scoliosis. *Spine (Phila Pa 1976)* 2011;37:957–65. doi:[10.1097/BRS.0b013e31823a012e](https://doi.org/10.1097/BRS.0b013e31823a012e).
- [14] Hill DL, Berg DC, Raso VJ, Lou E, Durdle NG, Mahood JK, et al. Evaluation of a laser scanner for surface topography. In: Tanguy A, Peuchot B, editors. *Res. into spinal Deform*. 3. IOS Press; 2002. p. 90.
- [15] Pazos V, Chieriet F, Danserau J, Ronsky J, Zernicke RF, Labelle H. Reliability of trunk shape measurements based on 3-D surface reconstructions. *Eur Spine J* 2007;16:1882–91. doi:[10.1007/s00586-007-0457-0](https://doi.org/10.1007/s00586-007-0457-0).
- [16] Stoler S, Baransi H, Givon U, Dvir Z. 3-D geometric imaging of the trunk in normal adolescents and age-matched patients impaired with idiopathic scoliosis: selected effects of conservative intervention according to Schroth. *Scoliosis* 2013;8:O20. doi:[10.1186/1748-7161-8-S1-O20](https://doi.org/10.1186/1748-7161-8-S1-O20).
- [17] Komeili A, Westover L, Parent EC, El-Rich M, Adeeb S. Correlation between a novel surface topography asymmetry analysis and radiographic data in scoliosis. *Spine Deform* 2015;3:303–11. doi:[10.1016/j.jspd.2015.02.002](https://doi.org/10.1016/j.jspd.2015.02.002).
- [18] Hill S, Franco-Sepulveda E, Komeili A, Trovato A, Parent E, Hill D, et al. Assessing asymmetry using reflection and rotoinversion in biomedical engineering applications. *Proc Inst Mech Eng Part H J Eng Med* 2014;228:523–9. doi:[10.1177/0954411914531115](https://doi.org/10.1177/0954411914531115).
- [19] Ho C, Parent E, Watkins E, Moreau M, Hedden D, El-Rich M, et al. Asymmetry assessment using surface topography in healthy adolescents. *Symmetry (Basel)* 2015;7:1436–54. doi:[10.3390/sym7031436](https://doi.org/10.3390/sym7031436).
- [20] Hocquet A, Cornelis F, Jirou A, Castaings L, de Sèze M, Hauger O. Patient-specific 3D models created by 3D imaging system or bi-planar imaging coupled with Moiré-Fringe projections: a comparative study of accuracy and reliability on spinal curvatures and vertebral rotation data. *Eur Spine J* 2016. doi:[10.1007/s00586-016-4659-1](https://doi.org/10.1007/s00586-016-4659-1).
- [21] Hong A, Jaswal N, Westover L, Parent EC, Moreau M, Hedden D, et al. Surface topography classification trees for assessing severity and monitoring progression in Adolescent Idiopathic Scoliosis (AIS). *Spine (Phila Pa 1976)* 2016;1. doi:[10.1097/BRS.0000000000001971](https://doi.org/10.1097/BRS.0000000000001971).
- [22] Knott P, Sturm P, Lonner B, Cahill P, Betsch M, McCarthy R, et al. Multicenter comparison of 3D spinal measurements using surface topography with those

- from conventional radiography. *Spine Deform* 2016;4:98–103. doi:[10.1016/j.jspd.2015.08.008](https://doi.org/10.1016/j.jspd.2015.08.008).
- [23] Komeili A, Westover LM, Parent EC, Moreau M, El-Rich M, Adeeb S. Surface topography asymmetry maps categorizing external deformity in scoliosis. *Spine J* 2014;14:973–83 e2. doi:[10.1016/j.spinee.2013.09.032](https://doi.org/10.1016/j.spinee.2013.09.032).
- [24] Komeili A, Westover L, Parent EC, El-Rich M, Adeeb S. Monitoring for idiopathic scoliosis curve progression using surface topography asymmetry analysis of the torso in adolescents. *Spine J* 2015;15:743–51. doi:[10.1016/j.spinee.2015.01.018](https://doi.org/10.1016/j.spinee.2015.01.018).
- [25] Michoński J, Walesiak K, Pakuła A, Glinkowski W, Sitnik R. Monitoring of spine curvatures and posture during pregnancy using surface topography—case study and suggestion of method. *Scoliosis Spinal Disord* 2016;11:31. doi:[10.1186/s13013-016-0099-2](https://doi.org/10.1186/s13013-016-0099-2).
- [26] Parent E, Watkins E, Emrani M, Hill D. Differences in measures of full-torso surface topography among healthy teenagers are independent of growth indicators. *Scoliosis* 2010;5:09. doi:[10.1186/1748-7161-5-S1-09](https://doi.org/10.1186/1748-7161-5-S1-09).
- [27] Teeter MG, Naudie DDR, Charron KD, Holdsworth DW. Three-dimensional surface deviation maps for analysis of retrieved polyethylene acetabular liners using micro-computed tomography. *J Arthroplasty* 2010;25:330–2. doi:[10.1016/j.arth.2009.11.001](https://doi.org/10.1016/j.arth.2009.11.001).
- [28] 3D Systems Geomagic Control X Software Broucher., 3D Systems, North Carolina, USA; 2016.
- [29] Rathnayaka K, Momot KI, Noser H, Volp A, Schuetz Ma, Sahama T, et al. Quantification of the accuracy of MRI generated 3D models of long bones compared to CT generated 3D models. *Med Eng Phys* 2012;34:357–63. doi:[10.1016/j.medengphy.2011.07.027](https://doi.org/10.1016/j.medengphy.2011.07.027).
- [30] Rathnayaka K, Sahama T, Schuetz Ma, Schmutz B. Effects of CT image segmentation methods on the accuracy of long bone 3D reconstructions. *Med Eng Phys* 2011;33:226–33. doi:[10.1016/j.medengphy.2010.10.002](https://doi.org/10.1016/j.medengphy.2010.10.002).
- [31] Wolf PR, DeWitt BA, Wilkinson BE. *Elements of photogrammetry with application in GIS*. 4th ed. McGraw-Hill Education; 2014.
- [32] Izatt MT, Bateman GR, Adam CJ. Evaluation of the iPhone with an acrylic sleeve versus the Scoliometer for rib hump measurement in scoliosis. *Scoliosis* 2012;7:14. doi:[10.1186/1748-7161-7-14](https://doi.org/10.1186/1748-7161-7-14).
- [33] Bonagamba GH, Coelho DM, Oliveira AS de. Inter and intra-rater reliability of the scoliometer. *Rev Bras Fisioter* 2010;14:432–8 doi:[S1413-35552010005000025](https://doi.org/10.1590/S1413-35552010005000025).
- [34] Côté P, Kreitz BG, Cassidy JD, Dzus AK, Martel J. A study of the diagnostic accuracy and reliability of the Scoliometer and Adam's forward bend test. *Spine (Phila Pa 1976)* 1998;23:796–802 discussion 803.